Imaging via subgrid upscaling and reverse time migration

Vitor Nunes and Susan E. Minkoff, The University of Texas at Dallas*

SUMMARY

Reverse time migration produces an image by cross-correlating the solution of the wave equation solved forward in time with the wave equation solved backwards in time. Solution of the wave equation can be computationally prohibitive for large subsurface regions. Therefore one typically combines a finite difference discretization of the wave equation with a parallel computing paradigm such as domain decomposition. Operator or subgrid upscaling is an alternate technique which produces a coarse scale solution of the wave equation that captures fine scale information. In the computationally intensive part of the algorithm one achieves ideal speedup without ghost cell allocation or communication. In this work we show the first images from reverse time migration (RTM) combined with operator upscaling. These upscaled images capture essentially the same velocity heterogeneities as RTM using the full fine grid solution.

INTRODUCTION

Seismic imaging and inversion are processes that involve repeated solution of the wave equation. For large simulation domains the solution of the wave equation can be prohibitively expensive and memory intensive. One of the most popular techniques for fast and accurate solution of the wave equation is domain decomposition or data parallelism applied to a finite difference discretization of the wave equation (see Pacheco (1997); Minkoff (2002)). This approach involves splitting up the total simulation domain into subdomains which are solved on different processors of a parallel machine. Grid information along subdomain boundaries must be shared between neighboring processors for the wave equation to be solved in each subdomain. This allocation of "ghost cells" on subdomain boundaries adds to memory requirements, and the communication required between processors is often the bottleneck in achieving perfect speedup in such simulations. As an alternative to this technique, Minkoff and her group have proposed and extensively studied a multiscale wave equation solution technique referred to as *subgrid or operator upscaling* which captures most of the fine grid solution details on a coarser domain (Vdovina et al. (2005); Korostyshevskaya and Minkoff (2006); Vdovina and Minkoff (2008); Vdovina et al. (2009)). The method does not require the domain have periodic boundary conditions nor does it assume an explicit scale separation (both common assumptions in homogenization theory, see Bensoussan et al. (1979); Bergman et al. (1985); Allaire (1992)). Numerical upscaling techniques have been studied most intensively for fluid flow (Chen et al. (2003); King and Williams (1996); Christie (1996)). Nonetheless, some references do exist for multiscale solution of the wave equation (in addition to the references from Minkoff's group, see for example, E et al. (2003); E and Engquist (2003); Chung et al. (2011); Gibson et al. (2014)).

Reverse time migration (RTM) cross correlates the solution of the wave equation from the physical sources with a back propagated wave field generated at the receivers. The source for the back propagated wave is the residual or difference between the measured or recorded data and the simulated wave field (Sun and McMechan (1988, 1991); Chattopadhyay and McMechan (2008)). Reflector locations are highlighted by this cross-correlation process. We present here the first results combining RTM with operator upscaling. Our forward wave field results from solving the wave equation using a parallel operator upscaling algorithm which does not require communication between processors and hence exhibits nearly ideal speedup without the usual i/o bottleneck of data parallelism.

THE OPERATOR UPSCALING ALGORITHM FOR ACOUSTICS

In this work we will focus on acoustics. However, the operator upscaling algorithm has also been analyzed in the context of flow (Arbogast et al. (1998); Arbogast and Bryant (2002); Arbogast (2003, 2004)) and 3D elastic wave propagation (Vdovina et al. (2009)). Our ultimate goal is to obtain a coarse solution (with fewer unknowns) which captures fine grid heterogeneities in the medium. Unlike traditional upscaling algorithms for fluid flow in which fine grid permeability is often averaged over a coarse block, the operator upscaling algorithm does not explicitly average any of the input parameters in the model (e.g., sound velocity or density in acoustics) but rather returns a *coarse grid solution* that captures small-scale heterogeneous features. In this particular 2D implementation we write the wave equation as a first order system in space by relating the gradient of pressure to a new unknown which is acceleration. The domain is decomposed into coarse and fine grid blocks with pressure living entirely on the fine grid and acceleration (a vector quantity) living on both the fine and coarse grid edges (see Figure 1). The upscaled quantity in this implementation is coarse acceleration. We note that other implementations are possible in which both pressure and acceleration are upscaled. In fact in Vdovina et al. (2009) all 6 unknown quantities are upscaled for the 3D velocity-displacement version of the elastic wave equation.

We now present the method. Let Ω be a two-dimensional domain with boundary Γ. We consider the acoustic wave equation in Ω written as a first-order system for acceleration $\vec{v}$ and pressure p:

$$\vec{v} = -\frac{1}{\rho}\nabla p \qquad \text{in } \Omega,$$

$$\frac{1}{\rho c^2}\frac{\partial^2 p}{\partial t^2} = -\nabla\cdot\vec{v} + f \qquad \text{in } \Omega,$$

DOI http://dx.doi.org/10.1190/segam2014-0817.1

Here c is the sound velocity, ρ is the density, and f is the source of acoustic energy.

The upscaling method was originally formulated in the context of the mixed finite element method applied to the flow equations (Arbogast et al. (1998)). Hence we begin by writing the system in variational form. In Vdovina et al. (2005) we describe how we exploit the equivalence between lowest order mixed finite elements and cell-centered finite differences to reduce the expensive part of the algorithm to a finite difference calculation typically used for solution of the wave equation. Nonetheless, we begin our description of the method by rewriting the system in weak form as follows: find $\vec{v} \in H_0(\mathrm{div};\Omega) = \{\vec{v} \in (L^2(\Omega))^2 : \nabla\cdot\vec{v} \in L^2(\Omega),$ and $\vec{v}\cdot\vec{\nu} = 0$ on $\Gamma\}$. and $p \in L^2(\Omega)$ such that

$$\begin{aligned} \langle \rho\vec{v}, \vec{u}\rangle &= \langle p, \nabla\cdot\vec{u}\rangle, \\ \left\langle \tfrac{1}{\rho c^2}\tfrac{\partial^2 p}{\partial t^2}, w\right\rangle &= -\langle \nabla\cdot\vec{v}, w\rangle + \langle f, w\rangle \end{aligned} \tag{1}$$

for all $\vec{u} \in H_0(\mathrm{div};\Omega)$ and $w \in L^2(\Omega)$.

The pressure space W is the space of piecewise discontinuous constant functions on the fine grid with nodes at the centers of the cells. We decompose acceleration into coarse and fine grid components $\vec{v} = \vec{v}^c + \delta\vec{v}$. Both the coarse and fine grid spaces for acceleration consist of piecewise linear vector functions living on the edges of the grid blocks (see Figure 1).

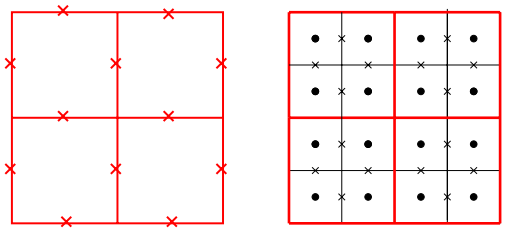

Figure 1: A 2×2 coarse grid with coarse acceleration unknowns and a corresponding 4×4 fine grid with subgrid unknowns. Pressures (denoted by dots) live at the centers of the cells. Acceleration (denoted by x's) lives on cell edges.

The upscaling process consists of two steps. First, we restrict to the subgrid test functions in System (1) and use the above decomposition to obtain a series of subgrid problems, one for each coarse grid block:

$$\begin{aligned} \langle \rho(\vec{v}^c + \delta\vec{v}), \delta\vec{u}\rangle &= \langle p, \nabla\cdot\delta\vec{u}\rangle, \\ \left\langle \tfrac{1}{\rho c^2}\tfrac{\partial^2 p}{\partial t^2}, w\right\rangle &= -\langle \nabla\cdot(\vec{v}^c + \delta\vec{v}), w\rangle + \langle f, w\rangle \end{aligned} \tag{2}$$

for all $\delta\vec{u} \in \delta V$, $w \in W$. The values of $\vec{v}^c$ are unknown at this stage, so we find the solution to the subgrid problem as a function of the coarse unknowns. Note, that the pressure is completely determined by System (2).

As stated above, Step 1 is the most computationally expensive part of the algorithm in that we must still solve for most of the original unknowns in the fine grid problem. However, two observations make this step cheap and ideally parallel. First, our choice of basis functions for pressure and acceleration allows us to solve this matrix system using explicit finite differences (Russell and Wheeler (1983)). Second, in Step 1 of the algorithm we impose an important simplifying condition on the space δV, namely,

$$\delta\vec{u}\cdot\vec{\nu} = 0 \quad \text{on the boundary of each coarse element.}$$

This is the only simplifying assumption in the definition of our method. It allows us to decouple the subgrid problems coming from different coarse-grid cells and is the reason why there is no communication between processors in the expensive first part of the algorithm. In fact, Step 1 is embarrassingly parallel!

The second step of the upscaling process uses $\delta\vec{v}$ and p to determine $\vec{v}^c \in V^c$ through solution of the upscaled coarse equation:

$$\langle \rho(\vec{v}^c + \delta\vec{v}(\vec{v}^c)), \vec{u}^c\rangle \quad = \quad \langle p, \nabla\cdot\vec{u}^c\rangle \tag{3}$$

for all $\vec{u}^c \in V^c$. Note that this portion of the process is fast as there are many fewer coarse grid unknowns than fine grid unknowns.

The problem is solved sequentially in time. We use second-order finite differences to approximate the time derivative in (2). First, we find the pressure on the current time level using the velocities and pressure from the previous time levels. Then we solve (2) and (3) for the subgrid and coarse velocities. The process then repeats for the next time step.

In the following table (reprinted from Vdovina et al. (2005)) we show a timing study for a numerical example with 3600×3600 fine grid blocks and 36×36 coarse grid blocks. The example was run for 20 time steps. Only the fine (or subgrid) solve (Step 1 of the algorithm) was parallelized. Step 2 (the coarse grid solve) was not parallelized; however, the coarse grid costs are insignificant compared to the cost of solving the subgrid problems. We note that we achieve essentially ideal (linear) speedup of the expensive part of the algorithm (the subgrid solve) with *no communication between processors*. On a single processor the cost of the upscaling is the same as solving the problem using standard finite differences.

number of processors	total time	subgrid problems	coarse problem	post-processing
1	29.70	29.69	0.00060	0.0026
2	15.46	15.38	0.00045	0.0711
4	7.63	7.56	0.00049	0.0707
6	5.23	5.14	0.00048	0.0749
8	4.37	4.26	0.00046	0.0896
12	3.07	2.94	0.00045	0.1150

Table 1: Speedup table for upscaling where all times are in seconds.

DOI http://dx.doi.org/10.1190/segam2014-0817.1

REVERSE TIME MIGRATION USING UPSCALING

As a starting point for imaging we employ the reverse time migration (RTM) method together with solution of the wave equation using operator upscaling. Our algorithm proceeds as follows:

1. Solve the forward problem using upscaling to obtain pressure p.
2. Calculate the residual $p_{res}(x_r,x_s,t,c) := p(x_r,x_s,t,c) - p_{obs}(x_r,x_s,t)$. where p_{obs} is the measured data.
3. Using this residual, back propagate the wave using upscaling to obtain ϕ:

$$\begin{cases} \vec{v} = -\dfrac{1}{\rho}\nabla\phi, \\ \dfrac{1}{\rho c^2}\dfrac{\partial^2\phi}{\partial t^2} = -\nabla\cdot\vec{v} + \displaystyle\sum_{r=1}^{N_r}\delta(\vec{x}-\vec{x_r})p_{res}(x_r,t) \end{cases}$$

4. Cross correlate p and ϕ via

$$\int_0^T \phi(\vec{x},t)p(\vec{x},t)dt.$$

to produce an image.

A NUMERICAL EXAMPLE

We will compare a reverse time migrated (RTM) image with upscaling against an RTM image without upscaling on a synthetic numerical experiment. The true image has a homogeneous background with velocity of 2500 m/s. We superimpose on this homogeneous background a series of diffractors with differing orientations and shapes. The diffractors all have higher velocities than the background medium with velocities ranging from 2700–3000 m/s. The density is assumed constant with a value of 1 g/cm^3. The domain contains 3000 $\times$ 3000 fine grid blocks (with mesh spacing of 1 m in x and z). We used 1000 receivers and 30 sources. Figure 2 shows the true image. The receivers are shown as a red horizontal bar located at 1500 m depth. The sources are shown as a yellow horizontal bar at the same depth as the receivers.

As our initial guess for migration we used the constant background velocity of 2500 m/s. For both the forward and backward solves we ran 5000 time steps with a time step size of .0001 s. The physical source is a Ricker wavelet in time convolved with a Gaussian function in space. We will show two sets of results. The first set comes from solving the wave equation without upscaling (the full fine grid solution). The second is the same experiment using upscaling. In the case of upscaling, we group together 10 fine blocks in x and 10 in z so that each coarse block contains 100 fine grid blocks.

Figure 3 shows the back propagated wave without upscaling at the final time. The back propagated wave with upscaling at this same time is shown in Figure 4. In the interest of efficiency, the cross-correlation is calculated using the trapezoid rule for integration with $dt = .005$ s. Thus every 50th time step

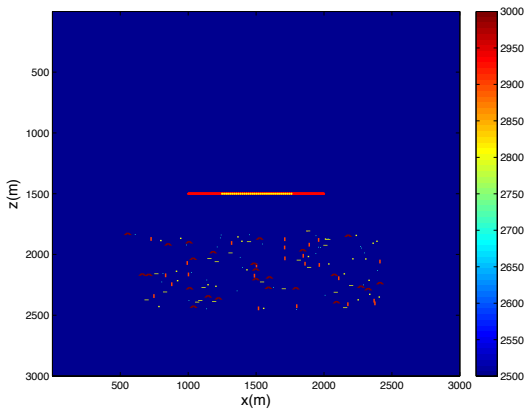

Figure 2: Original (true) image with the (1000) receiver locations shown as the red bar at 1500 m depth. The (30) sources are at the same depth and are indicated by the yellow bar. The background medium has a velocity of 2500 m/s. The diffractors have velocities ranging from 2700–3000 m/s.

is used in the cross correlation integral (sum). While a more sophisticated method such as checkpointing (Symes (2007)) is preferable, this simple integration scheme is enough for us to assess the accuracy of the upscaling method for imaging. Independent experiments were run for each of the 30 sources and the resulting images were summed to produce the final image.

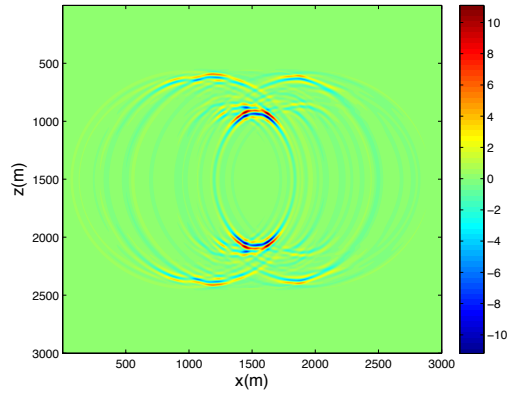

Figure 3: Full fine grid solution showing the back propagated wave at the final time (5000 time steps). The experiment that produced this image came from the source at (x,y)=(1500 m,1500 m).

Figure 5 is a zoomed-in view of the subset of the domain which we targeted for imaging. We are in the process of incorporating NPML boundary conditions into our numerical upscaling algorithm (see Cummer (2003); Hu and Cummer (2004); Hu et al. (2007)). However, for the experiments shown here we have chosen to use a large enough domain that we avoided artificial reflections from the computational domain boundaries. Figure 6 shows the cross-correlated image resulting from the

DOI http://dx.doi.org/10.1190/segam2014-0817.1

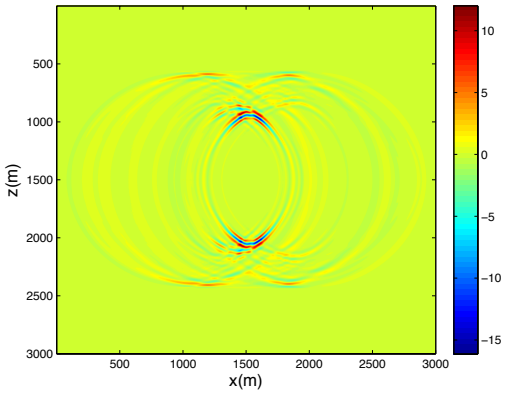

Figure 4: Back propagated wave at the final time (5000 time steps) for the experiment with upscaling. The source for this experiment is at (x,y)=(1500 m,1500 m).

full fine grid solution of the wave equation. Figure 7 shows the cross-correlated image gotten from using upscaling. In both of these figures the true solution (yellow diffractors) and image (light blue) are plotted together so that we see that both methods locate the diffractors in our target zone. The quality of the RTM results from the upscaled solution of the wave equation are remarkably similar to the image without upscaling. Clearly using more sources would improve the quality of the image. However, as a comparison between using upscaling and not, this small number of sources suffices.

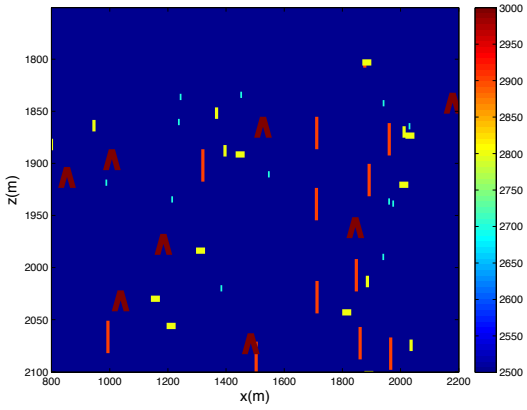

Figure 5: A zoomed in view of the true image.

CONCLUSIONS

We present in this paper the first results that combine operator upscaling for solution of the wave equation with reverse time migration. The operator upscaling algorithm solves the wave equation in two steps (a fine grid solve and then a coarse solve which uses the fine grid solution to reveal sub-wavelength solution heterogeneities). The only simplifying assumption in

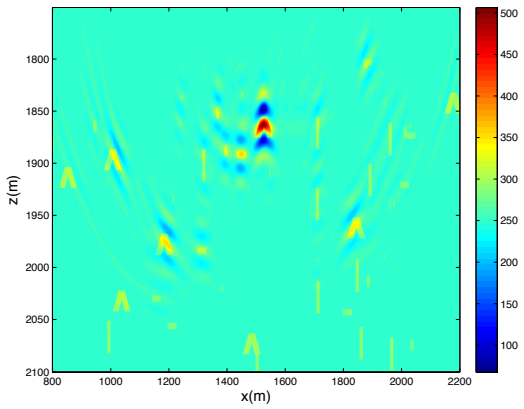

Figure 6: A zoomed in view of the reverse time migrated image using the full fine grid solution (no upscaling).

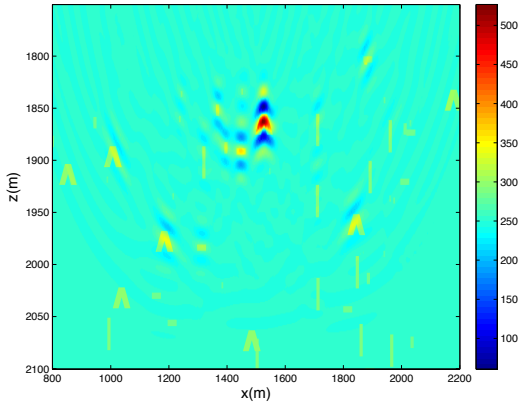

Figure 7: A zoomed in view of the reverse time migrated image using upscaling in which a factor of 10 fewer unknowns are used in both x and z.

the method is that in the first step (subgrid solve) we assume the coarse blocks are independent of neighboring coarse blocks so that the method exhibits ideal speedup with no communication between processors. Using upscaling as the wave equation solver for RTM, we see that the resulting images are remarkably similar to the images from the full fine grid solution of the wave equation. In future we plan to incorporate absorbing boundary conditions into the code and to test the algorithm on more realistic images and with differing amounts of upscaling.

ACKNOWLEDGMENTS

We wish to thank George McMechan of the University of Texas at Dallas and Bill Symes of Rice University for their help with the reverse time migration scheme.

DOI http://dx.doi.org/10.1190/segam2014-0817.1

http://dx.doi.org/10.1190/segam2014-0817.1

EDITED REFERENCES

Note: This reference list is a copy-edited version of the reference list submitted by the author. Reference lists for the 2014 SEG Technical Program Expanded Abstracts have been copy edited so that references provided with the online metadata for each paper will achieve a high degree of linking to cited sources that appear on the Web.

REFERENCES

Allaire, G., 1992, Homogenization and two-scale convergence: SIAM Journal on Mathematical Analysis, **23**, no. 6, 1482–1518, http://dx.doi.org/10.1137/0523084.

Arbogast, T., 2003, An overview of subgrid upscaling for elliptic problems in mixed form: American Mathematical Society, 21–32.

Arbogast, T., 2004, Analysis of a two-scale, locally conservative subgrid upscaling for elliptic problems: SIAM Journal on Numerical Analysis, **42**, no. 2, 576–598, http://dx.doi.org/10.1137/S0036142902406636.

Arbogast, T., and S. Bryant, 2002, A two-scale numerical subgrid technique for waterflood simulations: SPE Journal, **27**, 446–457.

Arbogast, T., S. Minkoff, and P. Keenan, 1998, An operator-based approach to upscaling the pressure equation: Computational Mechanics Publications, 405–412.

Bensoussan, A., J. Lions, and G. Papanicolaou, 1979, Asymptotic analysis for periodic structure: North Holland.

Bergman, D., J. Lions, G. Papanicolaou, F. Murat, L. Tartar, and E. Sanchez-Palencia, 1985, Les methodes de l'homogeneisation: theorie et applications en physique: Editions Eyrolles.

Chattopadhyay, S., and G. McMechan, 2008, Imaging conditions for prestack reverse-time migration: Geophysics, **73**, no. 3, S81–S89, http://dx.doi.org/10.1190/1.2903822.

Chen, Y., L. Durlofsky, M. Gerritsen, and X. Wen, 2003, A coupled local-global upscaling approach for simulating flow in highly heterogeneous formations: Advances in Water Resources, **26**, no. 10, 1041–1060, http://dx.doi.org/10.1016/S0309-1708(03)00101-5.

Christie, M., 1996, Upscaling for reservoir simulation: Journal of Petroleum Technology, **48**, no. 11, 1004–1010, http://dx.doi.org/10.2118/37324-MS.

Chung, E., Y. Efendiev, and R. Gibson, 2011, Multiscale finite element modeling of acoustic wave propagation: 81st Annual International Meeting, SEG, Expanded Abstracts, SEG, 2898–2903.

Cummer, S., 2003, A simple, nearly perfectly matched layer for general electromagnetic media: IEEE Microwave and Wireless Components Letters, **13**, no. 3, 128–140, http://dx.doi.org/10.1109/LMWC.2003.810124.

Gibson, R. Jr., K. Gao, E. Chung, and Y. Efendiev, 2014, Multiscale modeling of acoustic wave propagation in 2D media: Geophysics, **79**, no. 2, T61–T75, http://dx.doi.org/10.1190/geo2012-0208.1.

Hu, W., A. Abubakar, and T. Habashy, 2007, Application of the nearly perfectly matched layer in acoustic wave modeling: Geophysics, **72**, no. 5, SM169–SM175, http://dx.doi.org/10.1190/1.2738553.

Hu, W., and S. A. Cummer, 2004, The nearly perfectly matched layer is a perfectly matched layer: IEEE Antennas and Wireless Propagation Letters, **3**, no. 1, 137–140, http://dx.doi.org/10.1109/LAWP.2004.831077.

King, P., and J. Williams, 1996, Upscaling permeability: Error analysis for renormalization: Transport in Porous Media, **23**, no. 3, 337–354, http://dx.doi.org/10.1007/BF00167102.

Korostyshevskaya, O., and S. Minkoff, 2006, A matrix analysis of operator-based upscaling for the wave equation: SIAM Journal on Numerical Analysis, **44**, no. 2, 586–612, http://dx.doi.org/10.1137/050625369.

Minkoff, S., 2002, Spatial parallelism of a 3D finite difference, velocity-stress elastic wave propagation code: SIAM Journal on Scientific Computing, **24**, no. 1, 1–19, http://dx.doi.org/10.1137/S1064827501390960.

Pacheco, P., 1997, Parallel programming with MPI: Morgan-Kaufmann.

Russell, T., and M. F. Wheeler, 1983, The mathematics of reservoir simulation: SIAM.

Sun, R., and G. McMechan, 1988, Nonlinear reverse-time in-version of elastic offset vertical seismic profile data: Geophysics, **53**, 1295–1302, http://dx.doi.org/10.1190/1.1442407.

Sun, R., and G. McMechan, 1991, Full-wavefield inversion of wide-aperture SH- and Love wave data: Geophysical Journal International, **106**, no. 1, 67–75, http://dx.doi.org/10.1111/j.1365-246X.1991.tb04601.x.

Symes, W., 2007, Reverse-time migration with optimal check-pointing: Geophysics, **72**, no. 5, SM213–SM221, http://dx.doi.org/10.1190/1.2742686.

Vdovina, T., and S. Minkoff, 2008, An a priori error analysis of operator upscaling for the acoustic wave equation: International Journal of Numerical Analysis and Modeling, **5**, 543–569.

Vdovina, T., S. Minkoff, and S. Griffith, 2009, A two-scale solution algorithm for the elastic wave equation: SIAM Journal on Scientific Computing, **31**, no. 5, 3356–3386, http://dx.doi.org/10.1137/080714877.

Vdovina, T., S. Minkoff, and O. Korostyshevskaya, 2005, Operator upscaling for the acoustic wave equation: SIAM Journal on Multiscale Modeling and Simulation, **4**, no. 4, 1305–1338, http://dx.doi.org/10.1137/050622146.

Weinan, E., and B. Engquist, 2003, Multiscale modeling and computation: Notices of the American Mathematical Society, **50**, 1062–1070.

Weinan, E., B. Engquist, and Z. Huang, 2003, Heterogeneous multiscale method: A general methodology for multiscale modeling: Physical Review, **67**, 092101–1–092101–4.